International Journal on Artificial Intelligence Tools
Vol. 0, No. 0 (2000) 000—000

AN ALGORITHM FOR CANCER RECOGNITION OF ULTRASOUND IMAGES

E. A. YFANTIS, T. LAZARAKIS
University of Nevada,
Computer Science Department
Image Processing Laboratory
Las Vegas, NV 89154-4019

G. BEBIS
University of Nevada,
Computer Science Department
Reno,NV 89557

G. M. GALLITANO
West Chester University,
Department of Mathematics
West Chester, Pennsylvania 19383

Received (received date)
Revised (revised date)

An algorithm of cancer recognition of ultrasound images is developed in this paper. As we pointed out in our previous work, in order for cancer to survive it develops its own blood supply system, which is different than the supply system of normal tissue. The velocity of the blood flowing through the cancerous blood vessels is different than the velocity of the blood flowing through blood vessels of normal tissue. Due to this fact the ultrasound signal is absorbed differently in the cancerous areas than in the normal tissue areas. The energy of the signal, the continuity of the signal, the autocorrelation function and frequency domain properties are different in the normal tissue than in cancerous tissue. All of these indicators are weighted here for the purpose of classifying the image of the tissue as being cancerous or non cancerous. Preliminary results based on limited number of ultrasound images show that our method has the ability to recognize cancer in ultrasound images.

Keywords: Ultrasound Image, Cancer detection, blood velocity, probabilistic modeling.

1. Introduction

Unlike such methods as X-rays, CAT-SCAN, cameras sensitive to radioactive material, and other methods which obtain images of sections of the human body

and are invasive due to radioactivity, ultrasound is noninvasive. In ultrasound the produced sound signal is directed via a probe to a section of the body. Part of the sound signal is absorbed, part of it is reflected back directly, and part of it bounces onto one or more points before is reflected back to the receiver. The received sound intensity is quantized usually on a gray scale between 0 and 255 and therefore transformed from the sound space to the image space. It is the image space signal that we operate on. The ultrasound signal is absorbed differently by the various parts of the body. Thus soft tissue reflects the signal differently than muscle, or bone. So the fact that ultrasound is noninvasive allows the medical doctor to obtain several images of the part of the body which is of particular interest; furthermore, the acquisition of multiple images from different angles also allows for a 3-D image reconstruction using stereo image algorithms. Due to the multiple reflections of the sound signal (scattering of the signal), significant noise is incorporated with the signal. If we obtain several images of the same tissue sections by stabilizing the instrument and the patient, then we can reduce the noise considerably. The changes in the noise component are positive and negative, and they are a result of the fluctuation of the voltage, the fact that the patient is not totally still, and due to the inability of the instrument to deliver two identical digital images (compared pixel by pixel), when the conditions remain constant. If k images from the same view of the part of the body are obtained, and for each pixel we discard the lowest and highest of the pixel values and we average the remaining k-2 values, then the noise will decrease since the positive and negative values of the noise will cross each other out, and the signal is the same for each replication. Furthermore the ultrasound is very inexpensive and therefore affordable by all medical practitioners. Due to the non-invasive nature of ultrasound no special precaution measures have to be taken. Also the logistics of storage and installation of ultrasound machines are easier than the CAT-SCAN, X-rays, and others, since ultrasound machines are smaller, and lighter. An area of an ultrasound image of a prostate tissue can be classified as hypoechoic, isoechoic, or hyperechoic, depending on the intensity of the pixels in the area. Hypoechoic are the areas with relatively low pixel values, isoechoic the areas with pixel values about equal to the average pixel value of the image, and hyperechoic are areas with relatively high pixel values compared to the average pixel values of the image. In order to classify that a tissue area represented by an ultrasound image is cancerous or non cancerous first we classify the area as hypoechoic, isoechoic, hyperechoic or as a mixture of more than one type. Second, if it is a mixture we separate the sections and we investigate each section independently from the other(s). A vector of attributes are defined for each area to be recognized as cancerous or non cancerous. Subsequently a distance measure between the vector of attributes of the area of interest and two predefined centroids for that type of tissue, one for the cancerous and one for the noncancerous, are obtained. If the distance from the noncancerous centroid is smaller than that of the cancerous centroid, then the section of the image is classified as cancerous, otherwise if the distance between the section of the image attributes and the cancerous

centroid is smaller then the image is classified as cancerous. Our algorithm classifies correctly if the section of the tissue represented by the ultrasound image has cancer and we classify it as having cancer, or if the section of the tissue represented by the ultrasound image does not have cancer and we classify it as not having cancer. Our algorithm misclassified a section of a tissue represented by the ultrasound image if this section has cancer and the algorithm concludes that no cancer is present (false negative), or this section has no cancer and the algorithm concludes that cancer is present (false positive).

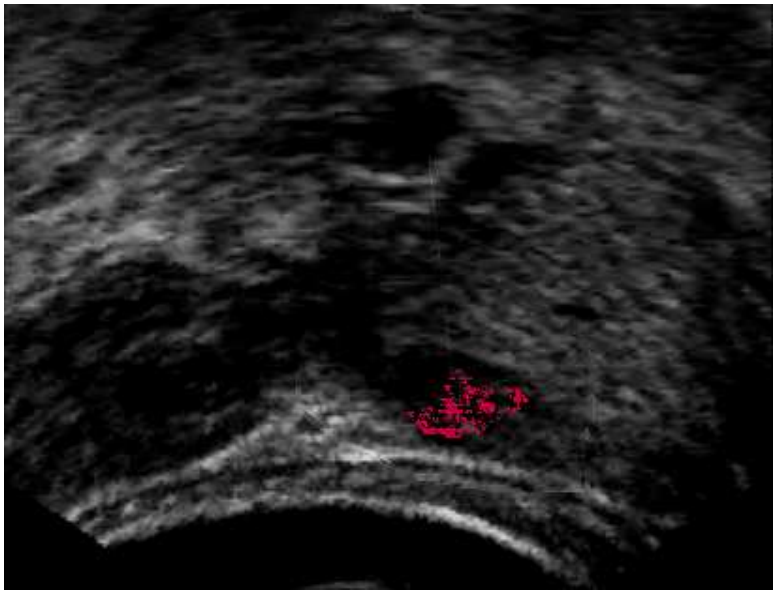

Fig. 1. Cancerous image.

The univariate distribution function for each one of the attributes used for recognition is obtained both as a histogram and as a mathematical function with the appropriate parameters. Furthermore the variance covariance matrix of the multivariate distribution of all the attributes is estimated. Also the centroid of the distribution in the multidimensional space is computed. Although the distribution of each one of the attributes is not normal, which implies that their multivariate distribution is also not normal, the distribution of their centroid is normal due to the extension of the central limit theorem to the multivariate space. The normalized cross-correlation function between attributes is scale independent and expresses the structural characteristics of the section of the image that the data was obtained from. The principal component analysis of the attributes used produces eigenvectors with directions depended on presence or absence of cancer in the tissue. Research related to this area is sparse and some of the papers are [1], [2], [3], [4], [5], [6], [7]. The

attributes considered here are the mean of the section of the tissue, the range, the estimated parameters of the probability distribution function of the autocorrelation function with lag one, and the first ten components of the cepstra.

2. The Recognition Algorithm

In our previous work we considered a sample support of 20 by 20 pixels; here we consider every pixel as the center of a square with side 21 pixels. Our theory is that cancer creates discontinuities in the tissue. In order for cancer to survive it develops its own blood supply system which is different than the supply system of normal tissue. The velocity of the blood flowing through the cancerous blood vessels is different than the velocity of the blood flowing through blood vessels of normal tissue. Due to this fact the ultrasound signal is absorbed differently in the cancerous areas than in the normal tissue areas. The energy of the signal, the continuity of the signal, autocorrelation function, frequency domain properties, are different in the normal tissue than in cancerous tissue. All these indicators are weighted here for the purpose of classifying the image of the tissue as being cancerous or non cancerous. The discontinuities alter the probability distribution of the autocorrelation function. The distribution of the autocorrelation function of a cancerous tissue (explained below) is somewhere between that of independent random variables and the distribution of the autocorrelation function of an image representing healthy tissue. Notice that the normalized autocorrelation function is scale independent. The distributions of the pixels in a neighborhood representing cancerous tissue is shifted towards the small values. This probability distribution function is modeled here using a gamma probability distribution function with parameters α and β. For the case of cancerous area the parameter α is very close to one, so the distribution function approaches the exponential probability distribution function. The gamma probability distribution function is of the form

$$f(x) = \frac{x^{\alpha-1} e^{\frac{-x}{\beta}}}{\beta^{\alpha}\Gamma(\alpha)} \tag{1}$$

where $\alpha > 0$, $\beta > 0$. The mean μ of the above distribution is $\mu = \alpha\beta$ and the variance $\sigma^2 = \alpha\beta^2$, estimates of the parameters $\alpha > 0$, $\beta > 0$, can be obtained using the method of moments. Let $\hat{\mu}$ be the estimate of the mean and $\hat{\sigma^2}$ be the estimate of the variance. $\hat{\mu} = \hat{\alpha}\hat{\beta}$ and $\hat{\sigma^2} = \hat{\alpha}\hat{\beta}^2$. From the above equations we obtain

$$\hat{\alpha} = \frac{\hat{\mu}^2}{\hat{\sigma^2}} \tag{2}$$

$$\hat{\beta} = \frac{\hat{\sigma^2}}{\hat{\mu}} \tag{3}$$

The parameter α is scale independent.

For hypoechoic areas with cancer $\hat{\alpha} = 1$, and $\hat{\beta} = \hat{\sigma}$

Lemma 1.

Let $X_1, X_2, X_3, ..., X_n$ be independent identically distributed random variables with mean *zero* and variance σ_X^2 then the distribution of the random variable $Y = X_i X_{i+k}$ has mean *zero* and variance equal to $\sigma_Y^2 = \sigma_X^4$.

Proof

The mean $\mu_Y = E(X_i X_{i+k}) = E(X_i)E(X_{i+k}) = 0$. The variance of Y is

$$\sigma_Y^2 = E(Y^2) = E(X_i^2)E(X_{i+k}^2) = \sigma_X^4 \tag{4}$$

As we see here the variance is independent of the space lag.

Theorem 1.

Let $X_1, X_2, X_3, ..., X_n$ be a sequence of random numbers obtained from a wide sense stationary random process with mean *zero*, and variance σ_X^2. Let also the space lag between X_i and X_{i+1} be fixed, and denoted by ΔX. Then the random variable $Y = X_i X_{i+k}$ has mean positive and depended on the lag k. As k increases the mean of Y approaches to *zero*. The variance $\sigma_Y^2 = E(X_{i+k}^2 X_i^2) - R^2(k)$ and $E(X_i^4) > \sigma_Y^2$, $E(X_i^4) > \sigma_{X_i}^4$

Proof

We have that

$$\begin{aligned} E(X_i^2 - E(X_i^2))^2 = E(X_i^4 \\ -2X_i^2 E(X_i^2) + E^2(X_i^2)) \end{aligned} \tag{5}$$

from the above equation we obtain

$$E(X_i^2 - E(X_i^2))^2 = E(X_i^4) - E^2(X_i^2) \tag{6}$$

or

$$E(X_i^2 - E(X_i^2))^2 = E(X_i^4) - \sigma_{X_i}^4 \tag{7}$$

From the above equation, since the left side is nonnegative we obtain

$$E(X_i^4) > \sigma_{X_i}^4 \tag{8}$$

Now

$$\begin{aligned} \sigma_Y^2 = E(X_i^2 X_{i+k}^2) \\ = E(X_{i+k}^2 X_i^2) - R^2(k) \end{aligned} \tag{9}$$

as the space lag increases the correlation between X_i, X_{i+k}, becomes smaller and tends to zero in which case

$$\sigma_Y^2 = E({X_i}^4) \tag{10}$$

on the other hand as k goes to zero

$$\sigma_Y^2 = E(X_i^4) - \sigma_{X_i}^4 \tag{11}$$

In Cancerous images σ_Y^2 is relatively large, and very close to $E({X_i}^4)$. The autocorrelation function for any lag has positive and negative values for cancerous images.

Theorem 2.

Consider the pixels X_{ij} and X_{ij+1}, let $Y = X_{ij} - X_{ij+1}$, then the $E(Y) = E(X_{ij} - X_{ij+1}) = 0$ and $\sigma_Y^2 = 2\sigma_X^2(1-\rho)$ and $\frac{\sigma_Y^2}{\sigma_X^2} = 2(1-\rho_1)$

$$\sigma_Y^2 = E(X_{ij} - X_{iJ+1})^2 = 2\sigma_X^2(1-\rho) \tag{12}$$

and

$$\frac{\sigma_Y^2}{\sigma_X^2} = 2(1-\rho_1) \tag{13}$$

Theorem 3

Now consider the pixel X_{ij} and the pixels X_{ij-1}, X_{ij+1}, X_{i-1j}, X_{i+1j} which have lag 1 from X_{ij} then consider $Y = X_{ij} - 0.25(X_{ij-1} + X_{ij+1} + X_{i-1j} + X_{i+1j})$ then the expected variable of Y is zero and the variance of Y is

$$\sigma_Y^2 = \sigma_X^2(1.25 - 2\rho_1 + 0.25\rho_2 + 0.5\rho_{\sqrt{2}} \tag{14}$$

Therefore

$$\frac{\sigma_Y^2}{\sigma_X^2} = 1.25 - 2\rho_1 + 0.25\rho_2 + 0.5\rho_{\sqrt{2}} \tag{15}$$

The estimate and distribution of $\sigma_{C_1}^2$ is different for cancerous and non cancerous areas. Furthermore the distribution of the normalized data $\frac{r_{ij}r_{i+1j}}{\sigma_r^2}$ is different for the cancerous and non cancerous areas.

From the above we infer that images with continuity and strong autocorrelation have normalized distribution of the lag product with variance which is greater than 1, where as the correlation decreases due to the discontinuities the normalized distribution of the lag product has variance close to 1. That implies if we consider the histogram of the normalized lag product multiplied by a factor 10, then in the non-cancerous areas we expect more energy namely bigger spread, than the cancerous areas.

Also from the above since the variance of the edges is higher when the continuity breaks down, cancerous areas are expected to have more edges and the inter-arrival time between edges is smaller. We define an activity level associated with a pixel to

the number of edges emanating from that pixel. Thus the activity level of cancerous areas is different than the activity level of non cancerous areas. The attributes associated with one area constitute a vector in the multivariate space. Based on a relatively large sample of hypoechoic normal areas and hypoechoic cancerous areas we calculate the centroid of the above defined attributes and their associated variance covariance matrices. For a new hypoechoic section of an image we estimate the above attributes and take the distance from the cancerous centroid and the noncancerous centroid. We classify the section of the image as cancerous if the distance of the vector of attributes of the section has smaller distance from the cancerous centroid than the non cancerous centroid; otherwise we classify the section as non cancerous. The recognition can be achieved by calculating the principal components of the variance covariance matrices of the cancerous, non cacerous and test image-section, and then taking the Mahalanobis distance of the test image-section from the cancerous and noncancerous centroids.

1. The estimate of the parameters α, and β, of the probability distribution function.

2. The variance of the pixels within the block represents the energy of the block, and in general cancerous blocks have less energy than non cancerous blocks.

3. If

$$Y_{ij} = x_{ij} - \bar{x} \tag{16}$$

$$S_Y^2 = \frac{\sum_{i=1}^{21} \sum_{j=1}^{21} Y_{ij}^2}{411} \tag{17}$$

and

$$r_{ij} = \frac{Y_{ij}}{S_Y} \tag{18}$$

then the histogram of the autocorrelation function ρ_1 of r_{ij} depends on the presence of cancer or not in the block.

4. The autocorrelation function and the variance of the autocorrelation function is another indicator.

5. X_{ij} are the pixel values of the block. Let $Y_{ij} = x_{ij} - x_{ij+1}$ then $E(Y_{ij}) = 0$ and variance of Y_{ij} is $\sigma_Y^2 = 2\sigma_X^2(1 - \rho_1)$ and

$$\frac{\sigma_Y^2}{\sigma_X^2} = 2(1 - \rho_1) \tag{19}$$

The presence of cancer reduces the ρ_1 so the above ratio is larger for cancer than non-cancer.

6. If we consider the

$$Y_{ij} = x_{ij} - 0.25(x_{ij-1} + x_{ij+1} + x_{i-1j} + x_{i+1j}) \tag{20}$$

then

$$\frac{\sigma_Y^2}{\sigma_X^2} = 1.25 - 2\rho_1 + 0.25\rho_2 + 0.5\rho_{\sqrt{2}} \tag{21}$$

For noncancerous this is close to zero where for cancerous blocks is close to 1.

An area of interest can be classified as hypoechoic, hyperechoic, isoechoic, or, if it is a mixed area, can be divided into its basic component areas by estimating the mean pixel intensity and the range. All the attributes form a vector. If we consider a hypoechoic block with cancer, the we denote the vector of the above parameters for this block as

$$H = [H1, H2, H3, H4, H5, H6],$$

if the block is hypoechoic with no cancer the same parameters will be denoted as

$$h = [h1, h2, h3, h4, h5, h6].$$

For isoechoic bloch with cancer the vector of the above parameters will be denoted as

$$I = [I1, I2, I3, I4, I5, I6],$$

while for isoechoic with no cancer we will denote it a

$$i = [i1, i2, i3, i4, i5, i6].$$

Finally for hyperechoic we will denote the parameters for ablock with cancer as

$$X = [X1, X2, X3, X4, X5, X6],$$

and with no cancer

$$x = [x1, x2, x3, x4, x5, x6].$$

$$\Sigma_H = \begin{bmatrix} \sigma_{H1}^2 & C_{H1,H2} & C_{H1,H3} & C_{H1,H4} & C_{H1,H5} & C_{H1,H6} \\ C_{H1,H2} & \sigma_{H2}^2 & C_{H2,H3} & C_{H2,H4} & C_{H2,H5} & C_{H2,H6} \\ C_{H1,H3} & C_{H2,H3} & \sigma_{H3}^2 & C_{H3,H4} & C_{H3,H5} & C_{H3,H6} \\ C_{H1,H4} & C_{H2,H4} & C_{H3,H4} & \sigma_{H4}^2 & C_{H4,H5} & C_{H4,H6} \\ C_{H1,H5} & C_{H2,H5} & C_{H3,H5} & C_{H4,H5} & \sigma_{H5}^2 & C_{H5,H6} \\ C_{H1,H6} & C_{H2,H6} & C_{H3,H6} & C_{H4,H6} & C_{H5,H6} & \sigma_{H6}^2 \end{bmatrix}$$

We considered all the hypoechoic blocks which are know to have cancer and we computed the average of the above attributes, let us denote this by

$$\mu_H = [\mu_{H1}, \mu_{H2}, \mu_{H3}, \mu_{H4}, \mu_{H5}, \mu_{H6}].$$

Also for all the hypoechoic blocks with no cancer we computed the Σ_h, μ_h. Let

$$U = [U1, U2, u3, u4, u5, u6]$$

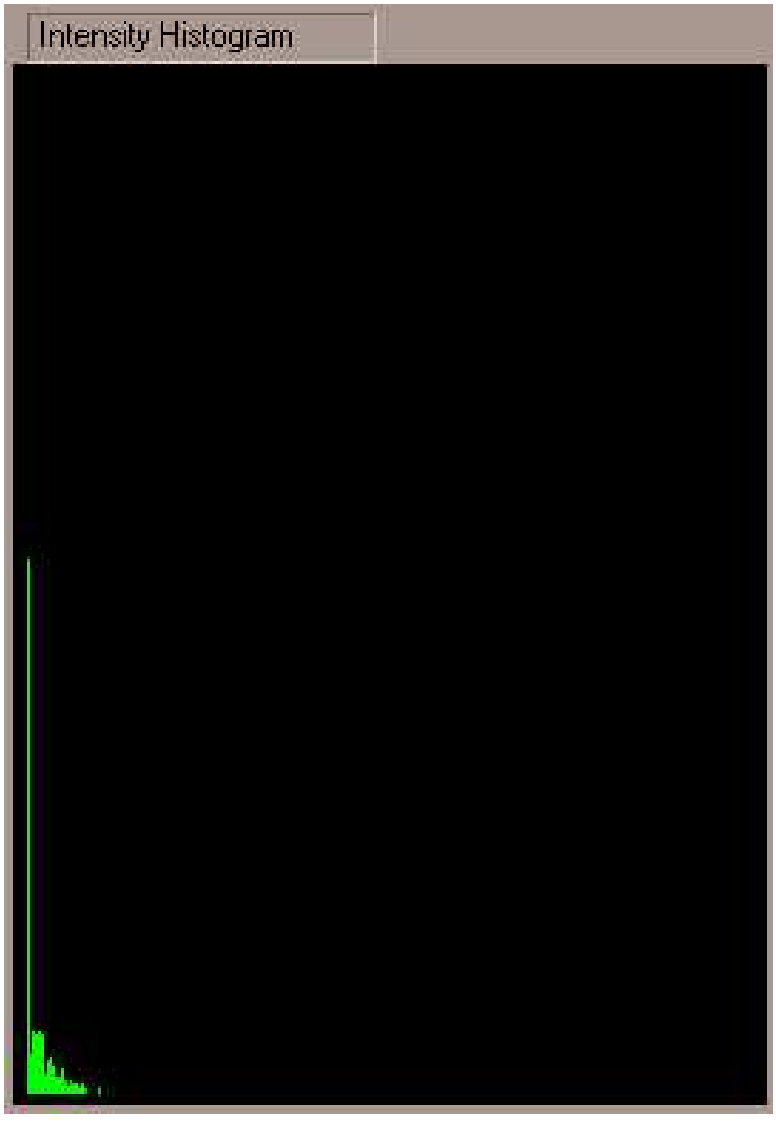

Fig. 2. Histogram of 21x21 block with cancer.

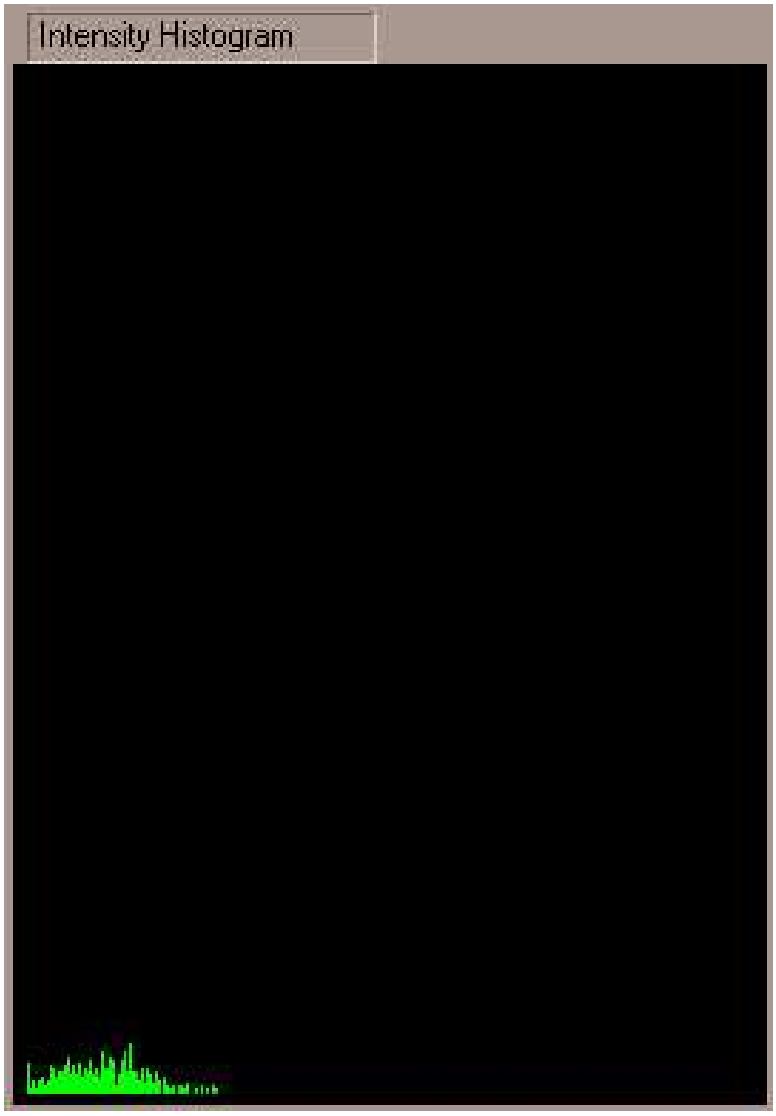

Fig. 3. Histogram of 21x21 block with no cancer.

be the attributes for an unknown hypoechoic block, then we compute the two Mahalanobis' distances:

$$(U - \mu_H)^T \Sigma_H^{-1} (U - \mu_H)$$

and

$$(U - \mu_h)^T \Sigma_h^{-1} (U - \mu_h)$$

We classify the block as cancerous or noncancerous based on which distance is the smaller. Thus if the distance from the cancerous hypoechoic is the smallest then the block is classified as cancerous otherwise as noncancerous. The same process applies to isoechoic and hyperchoic blocks.

Preliminary results based on limited number of ultrasound images show that our theory works. Each pixel of the tested images is the center of a 21x21 block. The stochastic attributes described above are computed for that block and based on the result, the block is classified as cancerous or non cancerous. Figure 4 shows a position of the 21x21 block. The moving block intellectually is similar to the needle testing except that the moving block is non invasive. Figure 1 shows the part of the image that has cancer based on our algorithm. Figures 2 and 3, show the histogram of a cancerous block and that of a non cancerous block, respectively.

Fig. 4. The 21x21 moving pixel spyglass has recognized cancer.

3. Summary and Conclusions

A cancer recognition algorithm of ultrasound prostate tissue was developed in this paper. The algorithm is based on calculating a number of attributes in the section of interest of the image and finding the distance in the multivariate space of the vector of attributes of the current section from two predetermined centroids, one for noncancerous regions of the same type and one obtained from cancerous regions of the same type (isoechoic, hypoechoic or hyperechoic). If the distance from the noncancerous centroid is smaller than the distance from the cancerous centroid, the region is classified as noncancerous, otherwise it is classified as cancerous.

[1] P. H. Carter, "Texture discrimination using wavelets," *SPIE*, Vol. 1567, pp. 432-438, 1991.

[2] R. N. Czerwinski, D. I. Jones, and W. D. O'Brian, "Edge Detection in Ultrasound Speckle Noise", *Computers in Cardiology, IEEE*, pp. 304-308, 1994.

[3] A. K. Jain, and F. Farrokhnia, "Unsupervised Texture Segmentation Using Gabor Filters", *Pattern Recognition,* Vol. 24, No. 12, pp. 1167-1186, 1991.

[4] T. Loch, E. A. Yfantis, et al, "Artificial Neural Network of Prostatic Transrectal Ultrasound," *The Prostate Journal*, Vol. 39, pp. 198-204, 1999a.

[5] E. A. Yfantis, V. Tsarev, C. Genberg, T. Loch, "Input Selection to Neural Network, Designed for Cancer Recognition on Prostate Tissue", *Proceedings of the ISCA, 5th International Conference*, pp. 178-181, 1996.

[6] E. A. Yfantis, M. Hiromoto, J. S. Cochran and G. M. Gallitano, "A Computer Algorithm for Cancer Recognition on Hypoechoic Ultrasound Images", *Proceedings of the ISCA, CAINE International Conference*, pp. 282-285, 1998.

[7] E. A. Yfantis, T. Lazarakis, G. Bebis, and G. M. Gallitano, "A Computer Algorithm for Cancer Recognition on Ultrasound Images of Prostate Tissue," *Proceedings of the 1999 IEEE International Conference on Information Intelligence and Systems*, Oct. 31-Nov. 3, Bethesda, Maryland, pp. 34-39, 1999b.